

Danthron Functions as a Retinoic X Receptor Antagonist by Stabilizing Tetramers of the Receptor*

Received for publication, July 20, 2010, and in revised form, November 5, 2010. Published, JBC Papers in Press, November 17, 2010, DOI 10.1074/jbc.M110.166215

Haitao Zhang^{‡1}, Rong Zhou^{§1}, Li Li[§], Jing Chen[‡], Lili Chen[‡], Chenjing Li[‡], Hong Ding[‡], Liang Yu[‡], Lihong Hu^{‡2}, Hualiang Jiang[‡], and Xu Shen^{‡§¶3}

From the [‡]State Key Laboratory of Drug Research, Shanghai Institute of Materia Medica, Chinese Academy of Sciences, 555 Zuchongzhi Road, Shanghai 201203, the [§]East China University of Science and Technology, 130 Meilong Road, Shanghai 200237, and the [¶]E-Institutes of Shanghai Municipal Education Commission, Shanghai Jiaotong University School of Medicine, 280 South Chongqing Road, Shanghai 200025, China

Retinoic X receptor (RXR) is a promising target for drug discovery against cancer and metabolic syndromes. Here, we identified a specific RXR α antagonist, danthron, from the traditional Chinese medicine rhubarb. Danthron repressed all tested RXR α -involved response element transcription, including the RXRE, PPRE, FXRE, and LXRE. Results from native PAGE and isothermal titration calorimetry (ITC)-based assays indicated that danthron bound to the tetrameric RXR α -LBD in a specific stoichiometric ratio, and such a binding could influence the corepressor SMRT affinity to the receptor. Additionally, a unique tetrameric structure of the apo-RXR α ligand-binding domain (LBD) was determined, which exhibited a larger tetramer interface and different ligand-binding pocket size compared with the one previously reported. Together with the biochemical and biophysical results, the determined crystal structure of danthron-soaked RXR α -LBD suggested a new mechanism for danthron antagonism to tetrameric RXR α . Moreover, the *in vivo* efficient improvement of insulin sensitivity by danthron was observed in diet-induced obese (DIO) mice. Thus, our findings were expected to supply new insights into the structural basis of RXR α antagonist for its further potential therapeutic application.

Retinoic X receptor (RXR),⁴ as a member of nuclear receptors (NRs), plays a central role in NR-regulated signaling pathways, for its obligate heterodimer partnership with almost one-

third of the family members, including peroxisome proliferator-activated receptor (PPAR), farnesoid X receptor (FXR), and liver X receptor (LXR) (1). RXR also self-associates into homodimer or homotetramer in the active or auto-repressed state (2). It is involved in a broad spectrum of biological processes such as cell growth, differentiation, metabolism, morphogenesis, and embryonic development (3, 4). Therefore, RXR has been considered as an important target for drug discovery in the treatment of cancer and metabolic syndromes (5, 6).

In structure, RXR exhibits typical features of nuclear receptor family. It primarily consists of a central DNA-binding domain and a carboxyl-terminal ligand-binding domain (LBD) (7). The multifunctional LBD is responsible for RXR dimerization, tetramerization, and ligand-induced activation (8). It is suggested that RXR exists predominately in inactive homotetramer in the absence of ligand *in vivo* and dissociates upon ligand binding to form homodimer or heterodimers with other NRs (9). To date, crystal structures of apoRXR α -LBD have been determined both in dimeric and tetrameric conformations (10, 11). The tetramer is formed with two dimers packed in a bottom-to-bottom manner (11). Binding of agonist such as RXR natural ligand 9-*cis* retinoic acid (9cRA) induces notable conformational changes in which the activation function-2 (AF-2) domain rotates and moves to its active position to seal off the ligand-binding pocket (LBP), thus recruiting coactivators to initiate transcription (12–14). Therefore, ligand-induced dissociation of the tetramer is considered to be the first step for RXR activation, and tetramer formation serves to sequester excess RXR into an inactive pool within the cell (15). However, the structural basis regarding RXR antagonist still remains elusive.

Small molecules that selectively regulate RXR signaling pathways are useful for their therapeutic application (7). RXR agonists have been reported to exhibit glucose-lowering, insulin-sensitizing, and anti-obesity efficiency in animal models of insulin resistance and type 2 diabetes (16). However, undesirable side effects such as hypertriglyceridemia and suppression of the thyroid hormone axis also exist (6). Currently, there have been

mediator for retinoid and thyroid receptor; NR, nuclear receptor; PPAR, peroxisome proliferator-activated receptor; FXR, farnesoid X receptor; LXR, liver X receptor; AF-2, activation function-2; 9cRA, 9-*cis* retinoic acid; LBP, ligand-binding pocket; RXRE, RXR-response element; PPRE, PPAR-response element; FXRE, FXR-response element; LXRE, LXR-response element.

* This work was supported by the State Key Program of Basic Research of China (Grants 2010CB912501, 2007CB914304, and 2009CB918502), the National Natural Science Foundation of China (Grants 30925040, 30890044, and 10979072), Key New Drug Creation and Manufacturing Program (2009ZX09301-001), the Science Foundation of Shanghai (Grant 08431902900), the E-Institutes of Shanghai Municipal Education Commission (Grant E09013), and the Foundation of Chinese Academy of Sciences (Grants KSCX2-YW-R-168 and SCX1-YW-02-2).

The atomic coordinates and structure factors (codes 3NSP and 3NSQ) have been deposited in the Protein Data Bank, Research Collaboratory for Structural Bioinformatics, Rutgers University, New Brunswick, NJ (<http://www.rcsb.org/>).

¹ Both authors contributed equally to this article.

² To whom correspondence may be addressed. Tel./Fax.: 86-21-50806918; E-mail: simmhulh@mail.shcnc.ac.cn.

³ To whom correspondence may be addressed. Tel./Fax.: 86-21-50806918; E-mail: xshen@mail.shcnc.ac.cn.

⁴ The abbreviations used are: RXR, retinoic X receptor; SPR, surface plasmon resonance; ITC, isothermal titration calorimetry; LBD, ligand-binding domain; DIO, diet-induced obese; SMRT, silencing

increasing numbers of reports on RXR antagonists, which are found to decrease body weight, plasma glucose, and insulin levels, while exhibiting few effects on food intake *in vivo* (17, 18).

In the current work, we identified a novel RXR α antagonist danthron, 1,8-dihydroxyanthraquinone (see Fig. 1A), from the traditional Chinese medicine rhubarb. This natural product repressed all of the tested RXR α -involved response elements transcription, including RXRE, PPRE, FXRE, and LXRE, without binding to the corresponding nuclear receptors, except RXR α . Results from the native PAGE indicated that danthron bound to the tetrameric RXR α -LBD and transformed the 9cRA-induced RXR α -LBD dimer to tetramer. ITC-based assay revealed that danthron bound to RXR α -LBD with a stoichiometric ratio of 1:2 (two ligands bound to one RXR α -LBD tetramer). Furthermore, danthron binding could influence the affinity of the silencing mediator for retinoid and thyroid receptor (SMRT) to the receptor. In addition, a unique homotetrameric structure of apoRXR α -LBD was discovered, which exhibited a larger tetramer interface and different ligand-binding pocket size, compared with the previously reported one. The danthron-interacting residues in LBP were determined by the crystal structure of danthron-soaked RXR α -LBD. These results have thus suggested a potential mechanism of RXR α -LBD tetramer stabilization by danthron. Furthermore, danthron exhibited an efficient improvement of insulin sensitivity in DIO mice, implying that danthron functioned as an insulin sensitizer *in vivo*. As a first report on RXR α -antagonist structural characterization, our work was expected to have provided a new insight of a novel antagonistic mode on the inactive RXR tetramer.

EXPERIMENTAL PROCEDURES

Materials—All the cell culture reagents were purchased from Invitrogen. The UAS-TK-Luc reporter was generously donated by Dr. Daniel P. Kelly (Washington University School of Medicine). The fusion constructs of pGAL4-RXR α -LBD, pGAL4-LXR α -LBD, pGAL4-FXR-LBD, and pGAL4-PPAR γ -LBD were generated using pGBKT7-RXR α -LBD, pcDNA3.1-LXR α , pET22b-FXR-LBD, and pcDNA3.1-PPAR γ (kindly provided by Dr. Gordon Hager, National Cancer Institute) as templates, respectively. The pGL3-pro-RXRE-Luc vector was constructed by inserting four DR1 sequences with XhoI-BglII sites. The pGL3-pro-LXRE-Luc plasmid was kindly provided by Dr. Peter A. Edwards (The Medicine Institute at University of California, Los Angeles), and pGL3-pro-FXRE-Luc vector was kindly provided by Dr. Majlis Hermansson (AstraZeneca, Mölndal, Sweden). The corepressor SMRT peptide was synthesized with the sequence NMGLEAIIRKALMGKY based on the published results (19).

Luciferase Assay—Mammalian one-hybrid test and transactivation experiment of RXR α -involved response element were performed using luciferase assay. HEK293T (human embryonic kidney) cells were cultured in DMEM supplemented with 10% FBS, 50 units/ml penicillin-streptomycin (Sigma) at 37 °C in a humidified atmosphere with 5% CO₂. Transient transfection was conducted using Lipofectamine 2000 (Invitrogen) according to the manufacturer's instructions. Briefly, 5 h after transfected with luciferase reporter vector

and *Renilla* luciferase vector pRL-SV40 (50 ng/well), cells were incubated with varied concentrations of compounds for another 24 h. Luciferase activities were measured using the Dual-Luciferase Assay System kit (Promega).

Protein Purification—Preparation of RXR α -LBD was performed according to the previously published approach (14). Briefly, the coding sequence of human RXR α -LBD (residues 221–458) was cloned to the vector pET15b, and *Escherichia coli* strain BL21 (DE3) was used for protein expression. The culture was induced with 0.5 mM isopropyl 1-thio- β -D-galactopyranoside and incubated at 25 °C for 6 h. His-tagged RXR α -LBD was purified with nickel-nitrilotriacetic acid resin (Qiagen), and the tag was then removed by thrombin (Novagen). The protein was further purified with Superdex 200 (Amersham Biosciences) and concentrated to 10 mg/ml.

SPR Technology-based Assay—Binding affinity of danthron toward RXR α -LBD was assayed with a BIACORE 3000 instrument (BIACORE) based on our previous report (20). All agents were purchased from GE Healthcare. Briefly, RXR α -LBD was immobilized onto a CM5 sensor chip according to the standard primary amine-coupling procedures. Danthron was serially diluted and injected into the channels at a flow rate of 20 μ l/min for 60 s, followed by disassociation for 120 s. BIAevaluation software (version 3.1; Biacore) was used to determine the equilibrium dissociation constant (K_D) of the compound.

Native PAGE Assay—The separating gel was prepared by mixing 4.8 ml of water, 2.7 ml of 30% acrylamide/0.8% bisacrylamide, 2.5 ml 5 M Tris-Cl, pH 8.8, 0.05 ml of 10% (w/v) ammonium persulfate, and 0.005 ml of *N,N,N',N'*-tetramethylethylenediamine. The stacking gel was prepared by mixing 3.3 ml of water, 0.67 ml of 30% acrylamide/0.8% bisacrylamide, 1 ml 0.5 M Tris-Cl, pH 6.8, 0.03 ml of 10% (w/v) ammonium persulfate, and 0.005 ml of *N,N,N',N'*-tetramethylethylenediamine. Phosphate gel buffer was prepared with 100 mM sodium phosphate and adjusted to pH 6.5. Albumin from bovine serum (66 kDa for monomer and 132 kDa for dimer) was purchased from Sigma and used as a native PAGE marker. A constant current of 30 mA was used for the 5-h polyacrylamide gel electrophoresis. All experiments were performed at 4 °C.

ITC Technology-based Assay—The thermodynamic properties of danthron binding to RXR α -LBD, corepressor SMRT peptide binding to apo-, or danthron-bound RXR α -LBD were determined using a VP-ITC titration calorimeter (MicroCal) in phosphate buffer at 25 °C. The heat of dilution was obtained by injecting danthron or SMRT into the same buffer and subtracted from the reaction before the fitting process.

Crystallization and Data Collection—RXR α -LBD crystals grew in the condition of 100 mM Tris-Cl, pH 6.5, 10% PEG4000, 5% glycerol. The complex crystal was obtained by soaking the RXR α -LBD crystal in the danthron-containing mother liquor with a mass ratio of 1:50. Diffraction data were collected at BL17U of Shanghai Synchrotron Radiation Facility in China and integrated with HKL2000 (21).

Structure Determination and Refinement—Phasing was performed by MOLREP (22). Structure refinement was carried out by Refmac5 (22) and CNS (23). Model building was performed by COOT (24). The quality of the final model was checked by PROCHECK (25). The statistics of the data collection

TABLE 1
Data collection and structure refinement statistics

	Apo-RXR α -LBD	RXR α -LBD-danthron
Data collection		
Space group	<i>P</i> 2 ₁ 2 ₁ 2	<i>P</i> 2 ₁ 2 ₁ 2
Cell dimensions		
<i>a</i> , <i>b</i> , <i>c</i> (Å)	114.83, 100.27, 47.16	115.03, 99.92, 47.20
α , β , γ	90°, 90°, 90°	90°, 90°, 90°
Resolution (Å)	29.72–2.90 (3.00–2.90) ^a	14.88–2.60 (2.69–2.60)
<i>R</i> _{sym} or <i>R</i> _{merge} ^b	0.158 (0.682)	0.128 (0.344)
<i>I</i> / σ <i>I</i>	4.7 (2.0)	4.8 (2.0)
Completeness (%)	90.7 (96.2)	95.5 (95.7)
Redundancy	9.3 (3.8)	4.5 (4.3)
Refinement		
Resolution (Å)	15.00–2.90	14.88–2.60
No. of reflections	11,445	16,495
<i>R</i> _{work} / <i>R</i> _{free} ^c	0.197/0.225	0.234/0.257
No. of atoms	3,019	3,113
Protein	2,985	2,992
Ligand	0	18
Water	34	103
<i>B</i> -factors (Å ²)	24.7	38.7
Protein	25.3	24.8
Ligand		41.9
Water	21.2	22.3
r.m.s.d. ^d		
Bond lengths (Å)	0.011	0.010
Bond angles	1.376°	1.235°
Ramachandran plot (%)		
Most favored regions	97.0	97.1
Allowed regions	3.0	2.9

^a Values in parentheses are for highest-resolution shell.

^b R_{sym} or $R_{\text{merge}} = \sum_h \sum_i |I_{hi} - \langle I_h \rangle| / \sum_h \sum_i I_{hi}$, where I_{hi} and $\langle I_h \rangle$ are the *i*-th and mean measurement of the intensity of reflection *h*, respectively.

^c $R_{\text{work}}/R_{\text{free}} = \sum_h |F_{o,h} - F_{c,h}| / \sum_h F_{o,h}$, where $F_{o,h}$ and $F_{c,h}$ are the observed and calculated structure factor amplitudes, respectively.

^d r.m.s.d., root mean square deviation.

and structure refinement were summarized in Table 1. All of the structure figures were prepared by PyMOL (26). Atomic coordinates and structure factors have been deposited to the Protein Data Bank under accession codes 3NSP and 3NSQ.

Insulin Tolerance Test—C57/BL6 male mice were obtained from Shanghai SLAC Laboratory Animal Co., Ltd. Mice were fed with a high fat diet for 3 months and treated with danthron (5 mg/kg) or vehicle orally for 8 weeks. The animals were then fasted for 6 h and then given intraperitoneal injection of insulin at 1.5 units/kg. Blood samples were analyzed at 15, 30, 45, 60, 90, and 120 min using Accu-Chek active blood sugar test meter (Roche Diagnostics). All of the animals received humane care, and the procedures in these experiments were performed according to the institutional ethical guidelines.

RESULTS

Danthron Was a Specific RXR α Antagonist—According to the SPR technology-based assay, danthron dose-dependently bound to RXR α -LBD with a K_D value of 6.2 μM (Fig. 1B). To further explore the effect of danthron on the transactivation of RXR α , a mammalian one-hybrid test was employed. As shown in Fig. 1C, danthron inhibited 9cRA-induced RXR α transactivation by IC₅₀ at 0.11 μM . Moreover, danthron repressed the transactivation of RXRE mediated by the RXR α :RXR α homodimer (Fig. 1D). Also, we examined the selectivity of danthron to several kinds of RXR α -involved heterodimers. The results showed that danthron dose-dependently repressed the transactivation of the relevant RXR α -involved response elements, including PPRE, FXRE, and LXRE, which are mediated by RXR α :PPAR γ , RXR α :FXR, and RXR α :LXR α heterodimers, respectively (Fig. 1, E–G). However, danthron

exhibited no activities to these nuclear receptors in mammalian one-hybrid test (Fig. 1, H–J). These results thus suggested that danthron exerted its transrepression activities on the RXR α homodimer and RXR α -involved heterodimers just through targeting RXR α , further addressing its selectivity to RXR α over other nuclear receptors.

Danthron Stabilized RXR α -LBD Tetramer and Influenced Corepressor SMRT Binding to Receptor—Currently, a few complex structures of antagonist-bound NRs have been reported, including the estrogen receptor (27), PPAR (19), glucocorticoid receptor (28), and retinoic acid receptor (29). All of these structures revealed a conserved dimeric fold, in which antagonists induced H12 adopting an alternative position to recruit corepressor. Here, we wondered whether danthron could induce dissociation of tetrameric RXR α -LBD to dimer. The results from size exclusion chromatogram and native PAGE assays suggested that purified RXR α -LBD existed in equilibrium of tetramer and dimer (Fig. 2, A and B). As an agonist, 9cRA changed this equilibrium to dimer (Fig. 2B), in accord with the crystal structure of 9cRA-induced dimeric RXR α -LBD (12). Interestingly, danthron was found to induce this equilibrium preferring to tetramer as indicated by the fact that the danthron-bound RXR α -LBD was mostly in tetrameric form (Fig. 2B). Moreover, danthron inhibited the 9cRA-induced RXR α -LBD dimer formation to tetramerization in a dose-dependent manner (Fig. 2C). These results thus suggested that danthron binding could stabilize RXR α -LBD tetramer. Different from other nuclear receptor antagonists that bound to dimeric NRs, danthron played its role on tetrameric RXR α .

To further clarify the stoichiometric ratio of danthron binding to RXR α -LBD, ITC experiment was performed. The K_D value of danthron bound to RXR α -LBD by ITC experiment was determined at 7.5 μM (Fig. 2D), in a good agreement with the SPR result. However, danthron was found to bind to the receptor in a ratio of 1:2 (Fig. 2D), different from the previously published reports on the equal ratio of receptor-ligand binding (12–14).

It was postulated that binding of the corepressor like the SMRT to nuclear receptors could be stabilized by antagonists (30, 31). Here, we evaluated the potential effects of danthron binding on SMRT peptide affinity to RXR α -LBD by ITC-based assay. As indicated in Fig. 2, E and F, SMRT peptide bound to unliganded RXR α -LBD in a ratio of 1:1, whereas danthron binding changed this ratio to 1:2. Therefore, the biochemical and biophysical results from the native PAGE and ITC experiments showed that danthron bound to the tetrameric RXR α -LBD in a specific stoichiometric ratio, and danthron binding could stabilize this tetramer and influenced the corepressor SMRT affinity to RXR α -LBD.

Apo-RXR α -LBD Exhibited a Unique Homotetrameric Conformation—To further elucidate the structural basis of danthron as a specific RXR α antagonist, we tried co-crystallization of RXR α -LBD with danthron but failed to get the crystals either in the presence or absence of corepressor SMRT peptide. Unexpectedly, we determined a unique homotetramer structure of apo-RXR α -LBD. As shown in Fig. 3A, the analyzed crystal structure of apo-RXR α -LBD generally

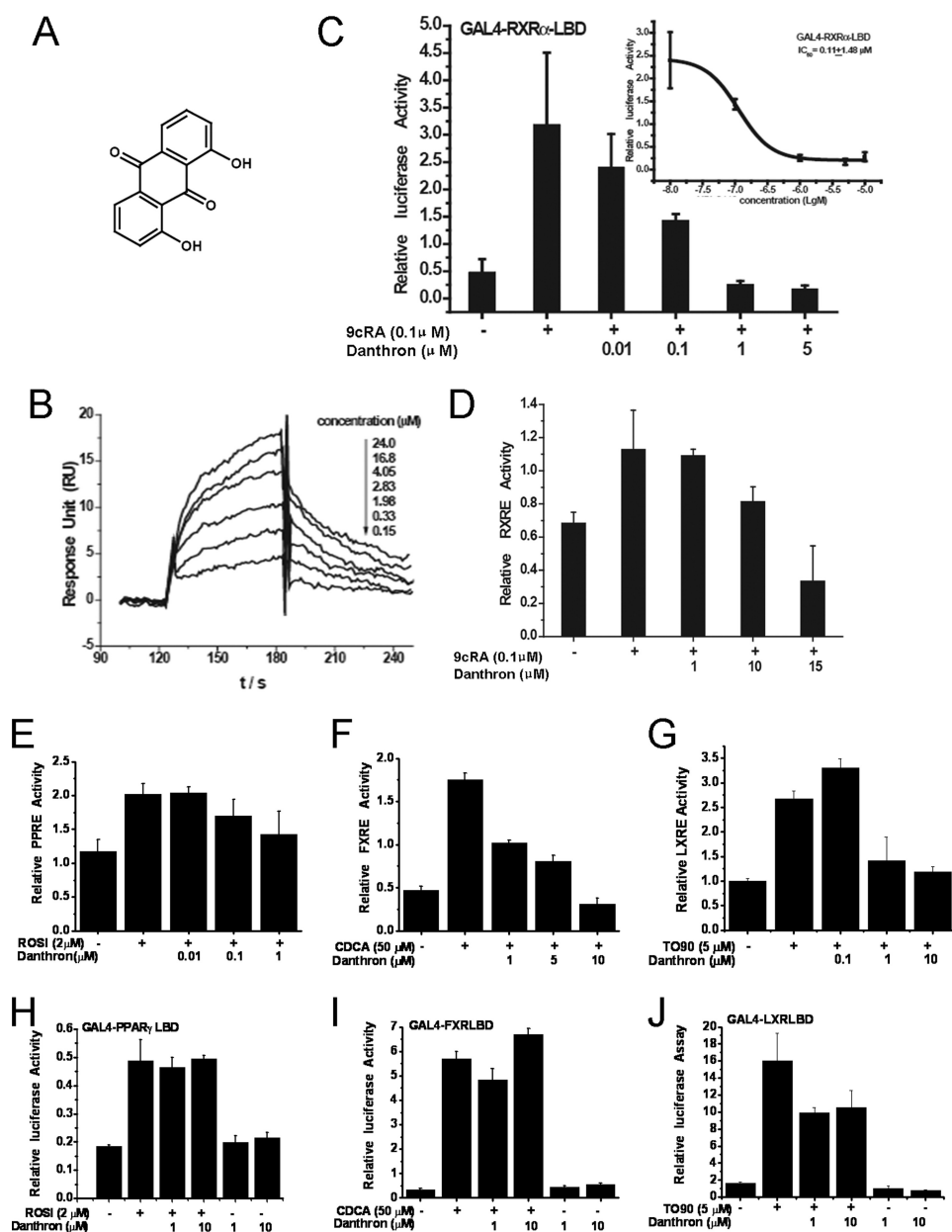


FIGURE 1. Danthron was a specific RXR α antagonist. *A*, chemical structure of danthron. *B*, danthron specifically bound to RXR α -LBD as evaluated by SPR technology-based assay. *C*, danthron antagonized 9cRA-stimulated transactivation of Gal4-RXR α -LBD in a dose-dependent manner by mammalian one-hybrid assay. The half-maximal inhibitory concentration (IC_{50}) was indicated. *D*, danthron antagonized the transactivation of RXRE mediated by the RXR α :RXR α homodimer. *E*, danthron antagonized the transactivation of PPARE mediated by the RXR α :PPAR γ heterodimer. *F*, danthron antagonized the transactivation of FXRE mediated by the RXR α :FXR heterodimer. *G*, danthron antagonized the transactivation of LXRE mediated by the RXR α :LXR α heterodimer. *H*, danthron exhibited no activities to PPAR γ by mammalian one-hybrid assay. *I*, danthron exhibited no activities to FXR by mammalian one-hybrid assay. *J*, danthron exhibited no activities to LXR α by mammalian one-hybrid assay. PPAR γ agonist rosiglitazone (ROSI), LXR agonist TO901317 (TO90), and FXR agonist chenodeoxycholic acid (CDCA) were used as positive controls.

adopted a similar homotetrameric packing with two symmetric dimers combined in a bottom-to-bottom fashion compared with the previously reported one (11). However, superposition of these two tetrameric structures gave different packing modes (Fig. 3*B*). The two upper dimers overlapped well, whereas the lower dimer in our structure rotated along the tetramer axis (Fig. 3*B*). Further alignment among the symmetric dimers in these two tetramers and the previously reported RXR α -LBD dimer (10, 11) showed a conserved core structure and variable C-terminal helices H11 and H12 (Fig. 3*C*). Moreover, unlike the dimeric RXR α -LBD with two iden-

tical chains, chains A and B in these two tetramers exhibited different conformations (Fig. 3*D*). It seemed that C-terminal swinging conformations existed in the apo-RXR α -LBD. As shown in Fig. 3*D*, in chain B of our structure, H11 moved apart from the core LBD and was shortened by half a turn, whereas H12 moved 9.5 Å horizontally and rotated 60° counterclockwise. Chain A also behaved similar movement and rotation, but to a lesser extent. Although H11 and H12 in different structures seemed to be in a swinging manner, their conformations were actually not flexible, considering that H12 positioned itself into the groove between H3' and H4'

Danthron Antagonizes RXR by Stabilizing Tetramers

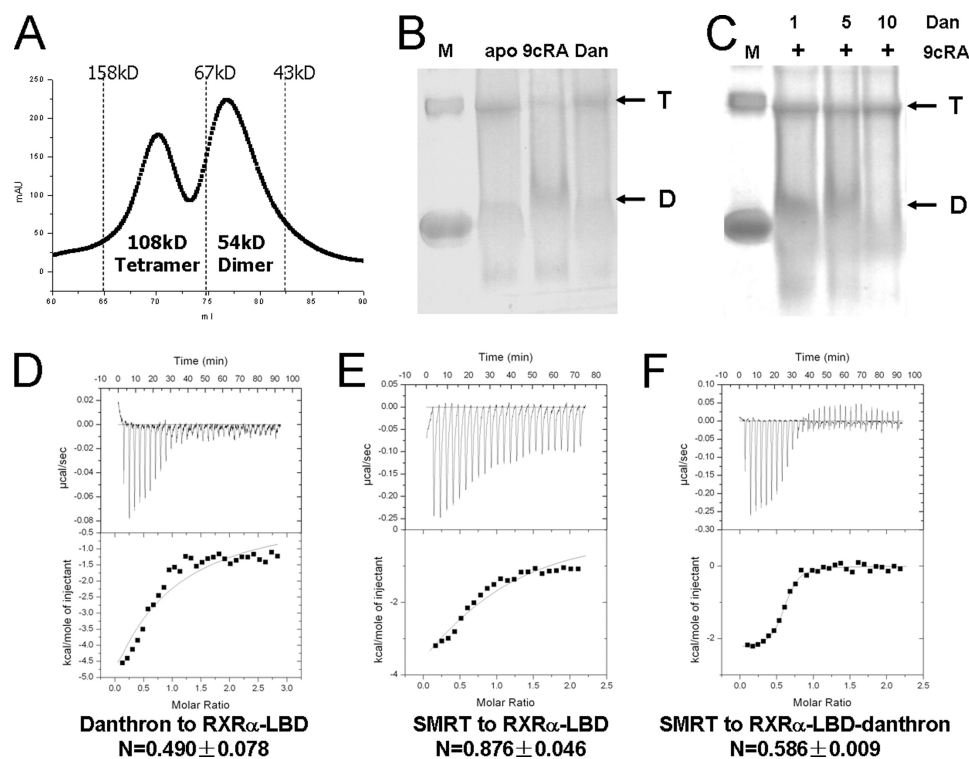


FIGURE 2. Danthron stabilized the RXR α -LBD tetramer and changed corepressor binding to the receptor. *A*, purified RXR α -LBD was in equilibrium of tetramers and dimers as indicated by size exclusion chromatogram assay. *B*, results from native PAGE showed that apo-RXR α -LBD existed in both tetramer (T) and dimer (D), whereas 9cRA-induced RXR α -LBD was mostly in dimer, and danthron-bound RXR α -LBD was mostly in tetramer. Albumin from bovine serum (66 kDa for monomer and 132 kDa for dimer) was used as marker (M). *C*, incubation of 9cRA-bound RXR α -LBD with an equal amount or 5- or 10-fold of danthron showed the transformation of RXR α -LBD from dimer to tetramer in a dose-dependent manner. *D*, ITC results showed that danthron (Dan) bound to RXR α -LBD in a molecular ratio of 1:2. *E*, ITC results showed that corepressor SMRT peptide bound to apo-RXR α -LBD in a stoichiometric ratio of 1:1. *F*, ITC results showed that corepressor SMRT peptide bound to danthron-bound RXR α -LBD in a stoichiometric ratio of 1:2.

from its neighbor dimer (Fig. 3A). The changes in C-terminal conformation for the apo-RXR α -LBD resulted in different sizes of LBP (Fig. 3E). The previously reported tetrameric RXR α -LBD had a slightly larger pocket on one side and a smaller one on the other compared with the dimeric RXR α -LBD (10, 11). However, chain B in our structure had an even larger pocket size, and chain A had the smallest size. It seemed that as the LBP in one side was enlarged, the pocket in the other may adjust itself by shrinking.

In addition, there were significant conformational changes on the tetramer interface, comparing our apo-RXR α -LBD structure with the reported structure (11). In the published structure, the H3/H3 interface was composed of the residues 264–269 of chain B and the residues 269–273 of chain A, the H11/H11 interface was constituted of Leu⁴³⁶ and Phe⁴³⁹ from each chain, and the AF-2/coactivator binding site interface was made up of Leu⁴⁵¹, Met⁴⁵, and Leu⁴⁵⁵ with helices 3 and 4 (11). Our results revealed that Leu⁴³⁶ and Phe⁴³⁹ in chain A and Phe⁴³⁸ in chain B constituted the H11/H11 interface (Fig. 3F). H11 of chain A also made additional hydrophobic interactions with Arg³⁰² in H4 and Trp³⁰⁵ in H5 of chain B. The AF-2 residues 451LMEM455 in chain A resembled the LXXLL motif of coactivators (underlined residues indicate a conserved sequence (11)) and interacted with Phe²⁷⁷, Lys²⁸⁴, and Val²⁹⁸ in chain B (Fig. 3G). These conformational changes in our structure made the two symmetric dimers adhere to each other burying 1475.8Å² of their surface, much larger than the

previously reported tetramer (1242.8Å²) (11). These results thus indicated that our determined apo-RXR α -LBD might be in a more stable state.

Crystal Structure of Danthron-bound RXR α -LBD—Although we failed to get the co-crystal of RXR α -LBD with danthron, the determined danthron-soaked crystal structure of tetrameric RXR α -LBD seemed to be valuable for elucidation of the ligand interacting information in the LBP. As shown in Fig. 4, A and B, the clear electron density was indicative of danthron existence. In addition, the binding stoichiometric ratio observed in the structure was in good accordance with the ITC results, where two ligands bound to one tetrameric RXR α -LBD.

Danthron was found to bind to the hydrophobic LBP by interacting with Phe³¹³ in H5, Ile³²⁴ and Leu³²⁶ in S1, Val³³² in S2, Val³⁴² and Phe³⁴⁶ in H7, and Phe⁴³⁷ in H11 (Fig. 4A). Danthron binding was further stabilized by forming hydrogen bonds with Lys⁴⁴⁰ (Fig. 4C). Interaction with danthron made Lys⁴⁴⁰ closer to the compound and induced an overturning of Phe⁴³⁹ in H11. Mutation of the conserved residue Phe⁴³⁹ on the tetramer interface was reported to abolish the ability of RXR to form tetramer (32). Upon danthron binding to RXR α -LBD, Phe⁴³⁹ might play an essential role in stabilizing this homotetramer. The residues involved in the hydrophobic interaction also adjusted themselves after danthron binding. As shown in Fig. 4C, the most significant conformational changes occurred on the β -sheets S1 and S2. To approach danthron, Leu³²⁶ in

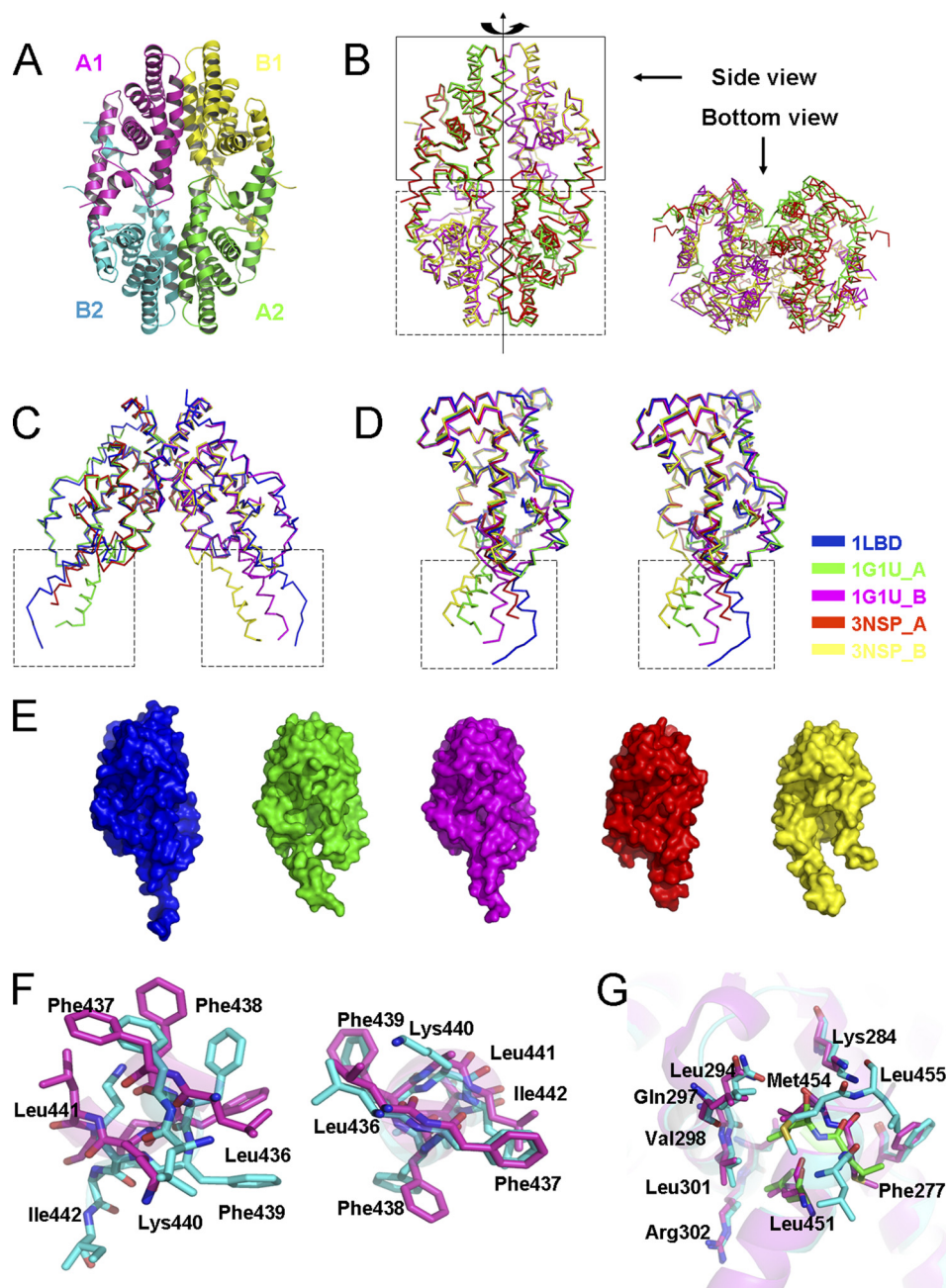


FIGURE 3. Apo-RXR α -LBD exhibited a unique homotetrameric conformation. *A*, overall structure of the current tetrameric RXR α -LBD shown in a ribbon diagram. Chains A and B and their symmetric chains were indicated. *B*, superposition of the current tetrameric RXR α -LBD (red and yellow) with the previously reported tetramer (Protein Data Bank code 1G1U, in green and magenta) showed different dimer packing. Upper dimers in the closed box adopted a similar conformation, but lower dimers in the dashed box did not overlap well due to its rotation along the tetrameric axis. *C*, superposition of the previous dimeric RXR α -LBD (Protein Data Bank code 1LBD) with the symmetric dimers from the current and previous tetramer showed identical dimer packing and C-terminal swinging conformation (in dashed box). *D*, superposition of chains from the current structure, previous RXR α -LBD dimer and tetramer in stereo view showed a conserved core structure and C-terminal swinging conformation (in dashed box). *E*, comparison of the ligand-binding pocket among the five chains mentioned above. Colors in *C*, *D*, and *E* were indicated. *F*, conformational changes of the residues were shown on the H11/H11 interface. *G*, conformational changes of the residues were shown on the AF-2/coactivator binding-site surface. The current structure was in cyan, and the previous tetramer was colored in magenta. Conserved residues in coactivator SRC-1 were shown in green.

S1 and Val³³² in S2 moved toward the ligand. This movement made the neighbor residues His³³¹ and His³³³ alter their conformations to get the whole β -sheet closer to danthron. Phe³¹³ and Arg³¹⁶ in H5 also shifted greatly. Arg³¹⁶ was the essential residue in the active RXR α -LBD structure by forming hydrogen bonds with RXR agonist 9cRA (12). All of these conformational changes of the hydrophobic residues led to the changes on the LBP electrostatic surface

(Fig. 4D). Because danthron was an anthraquinone type of compound with strong hydrophobic features in structure, changes on the LBP electrostatic surface were expected to facilitate danthron binding to the pocket. Moreover, the N-terminal part of H3 failed to bend toward the ligand as it did in the agonist-induced activation state, due to the steric hindrance from danthron (Fig. 4E). Although the LBP on both sides were open to solvent, danthron was

Danthron Antagonizes RXR by Stabilizing Tetramers

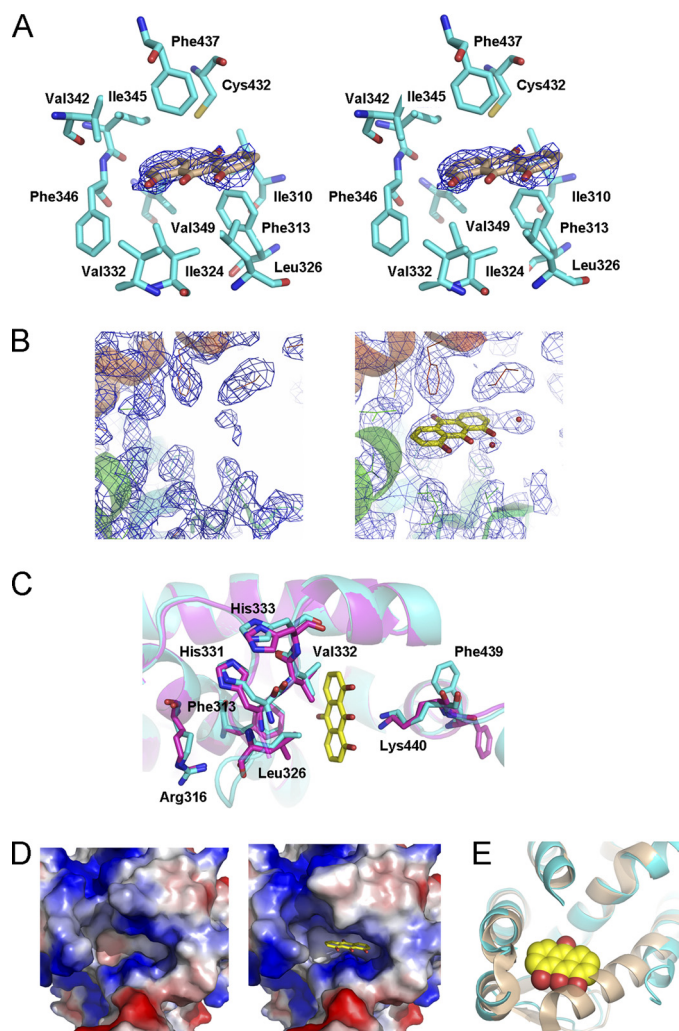


FIGURE 4. Crystal structure of danthron-bound RXR α -LBD. *A*, electron density of danthron (contoured at 1.0 σ level) was shown in stereo view. Hydrophobic residues in LBP were indicated in cyan sticks. *B*, $2F_o - F_c$ maps in LBP of apo- and danthron-soaked RXR α -LBD structures revealed a clear electron density of danthron. *C*, danthron binding induced conformational changes of LBP. Danthron-bound RXR α -LBD was in cyan, apo-RXR α -LBD was in magenta, and danthron was in yellow. *D*, danthron induced changes on the electrostatic surface of LBP. *E*, N terminus of H3 in danthron-bound RXR α -LBD structure (in cyan) failed to bend toward the ligand as it did in 9cRA-induced activation state (Protein Data Bank code 1FBY, in wheat), due to the steric hindrance from danthron.

found to bind to merely two chains of the tetramer as indicated in our determined crystal structure of danthron-soaked RXR α -LBD. The pocket of chain A was shrunken and not large enough for danthron binding. The binding stoichiometric ratio in the structure is in good accord with the ITC results (Fig. 2D).

Danthron Improved Insulin Sensitivity in DIO Mice—The insulin tolerance test result showed that danthron-treated diet-induced obesity mice exhibited lower glucose levels after insulin challenge, compared with the control vehicle-treated group (Fig. 5). Our results thereby suggested that danthron functioned as an insulin sensitizer *in vivo*.

DISCUSSION

Structural comparison of our determined apo-RXR α -LBD structure with the previously reported tetramer (11)

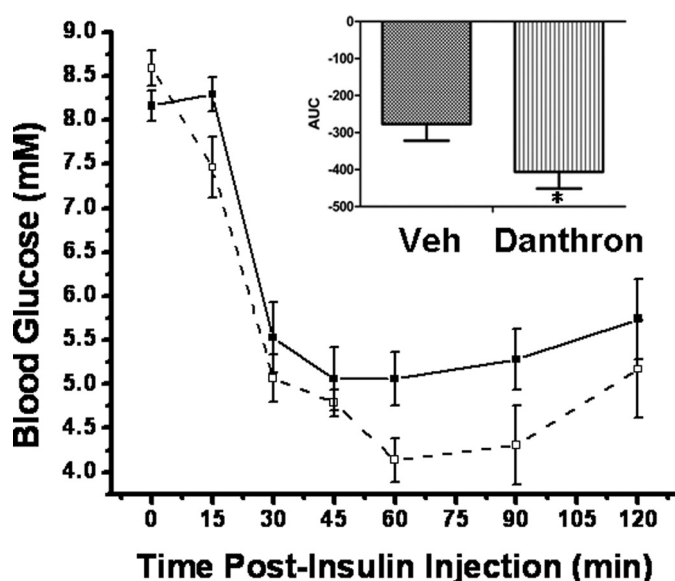


FIGURE 5. Danthron improved insulin sensitivity *in vivo*. In the insulin tolerance test, danthron-treated DIO mice showed lower glucose levels after insulin challenge, compared with the vehicle (Veh)-treated group. The area under curve of danthron-treated DIO mice exhibited a significant difference from that of the control group. Significant difference at $p < 0.05$; $n = 5$. (■, vehicle-treated group; □, danthron-treated group).

clearly showed that the conformational changes of C-terminal H12 in our structure were more substantial, which resulted in a larger tetramer interface and different LBP size (Fig. 3). It is tentatively suggested that our unique crystal packing might possibly attribute to the different crystallization conditions. As indicated, our crystals grew in a lower pH value of 6.5, different from that of 7.5 for the previous tetramer (11). Interestingly, dimeric RXR α -LBD crystal grew in a neutral pH of 7.0 (10). The physiological significance of these different conformations might be related to the competence of RXR for different ligands. RXR is known to distribute widely in various tissues with variable intracellular pHs (16). Therefore, RXR might probably adopt different conformations to accept different ligands, consequently forming heterodimers with different nuclear receptors to mediate different genes transcription, which was in accordance to the central position of RXR in the signaling pathways (1).

RXR was previously expected to exhibit similar antagonistic features to other nuclear receptors (7). However, in our work, the specific RXR antagonist danthron employs an alternative antagonistic mechanism on RXR α . By interacting with the residues on the essential helices H5 and H11, and β -sheets S1 and S2, danthron stabilizes RXR α -LBD in its inactive tetramer state, where the essential residue Phe⁴³⁹ on the tetramer interface might play an important part. Mutation of this conserved residue Phe⁴³⁹ on the tetramer interface was reported to abolish the ability of RXR to form tetramer (32). RXR exists predominately in inactive homotetramer *in vivo*, which is different from the other NRs (9); thus, it was not surprising to find an antagonist acting on this inactive tetramer. Because the agonist-induced dissociation of the tetramer is considered to be the first step of RXR activation, danthron plays its role at the

initial stage. Danthron arrests RXR α from rearrangement for transactivation, and the autorepression by homotetramer maintains RXR α in its inactive state. Therefore, the antagonism on the tetrameric RXR makes danthron distinguished from other antagonists on dimeric NRs.

In addition, our results from ITC-based assay for the first time indicated that the corepressor SMRT peptide had a binding affinity to the unliganded RXR α -LBD *in vitro*, although the mechanism involved in RXR repression by this corepressor is still not revealed. Moreover, binding of danthron was found to affect the corepressor SMRT affinity to the receptor.

Cell-based assays showed that danthron could inhibit RXR capability to transactivate reporter constructs driven by response elements for RXR α homodimer and all of the tested RXR α -containing heterodimers. Also, reversion of 9cRA-induced RXR α -LBD dimerization to tetramerization by danthron was observed in native PAGE (Fig. 2C). These results suggested that danthron-bound RXR α -LBD, as an inactive tetramer for transactivation, had no activity on the RXR-regulated gene transcriptions. Therefore, by stabilizing the tetrameric RXR α -LBD, danthron takes its effects on repressing all of the RXR α -involved transcriptions.

Danthron is an anthraquinone-type of compound isolated from the traditional Chinese medicine rhubarb. Rhubarb extracts have been proved to process promising antidiabetic and anticancer properties, although their detailed mechanisms remain unclear (33). One of the rhubarb extracts is rhein, which has an additional carboxyl group at the C3 site of danthron. Rhein was proved effective in the treatment of experimental diabetic nephropathy (34). Emodin, another main component of rhubarb, is an analog of danthron with the C3 and C6 sites substituted for methyl and hydroxyl groups, respectively. It was reported to have the competency to activate PPAR γ (35), and emodin-treated diabetic mice showed improved glucose tolerance and insulin sensitivity (36). Possessing a similar chemical structure to other components from rhubarb, danthron was thereby expected to display similar biological activities. Our insulin tolerance test experiment in DIO mice treated with danthron has revealed that this natural product functioned as an efficient insulin sensitizer *in vivo*.

Our results are expected to have provided new insights into the structural basis of RXR antagonists for their potential therapeutic application. The ability to improve insulin sensitivity has made danthron a promising lead compound for the development of antidiabetic drugs and supplied useful information for understanding the pharmacological mechanisms of rhubarb.

Acknowledgment—We thank BL17U of Shanghai Synchrotron Radiation Facility in China for data collection.

REFERENCES

1. Germain, P., Chambon, P., Eichele, G., Evans, R. M., Lazar, M. A., Leid, M., De Lera, A. R., Lotan, R., Mangelsdorf, D. J., and Gronemeyer, H. (2006) *Pharmacol. Rev.* **58**, 760–772
2. Kersten, S., Dong, D., Lee, W., Reczek, P. R., and Noy, N. (1998) *J. Mol. Biol.* **284**, 21–32
3. Mangelsdorf, D. J., Kliewer, S. A., Kakizuka, A., Umesono, K., and Evans, R. M. (1993) *Recent Prog. Horm. Res.* **48**, 99–121
4. Giguère, V. (1994) *Endocr. Rev.* **15**, 61–79
5. Tanaka, T., and De Luca, L. M. (2009) *Cancer Res.* **69**, 4945–4947
6. Pinaire, J. A., and Reifel-Miller, A. (2007) *PPAR Res.* **2007**, 94156
7. de Lera, A. R., Bourguet, W., Altucci, L., and Gronemeyer, H. (2007) *Nat. Rev. Drug Discov.* **6**, 811–820
8. Gronemeyer, H., Gustafsson, J. A., and Laudet, V. (2004) *Nat. Rev. Drug Discov.* **3**, 950–964
9. Kersten, S., Kelleher, D., Chambon, P., Gronemeyer, H., and Noy, N. (1995) *Proc. Natl. Acad. Sci. U.S.A.* **92**, 8645–8649
10. Bourguet, W., Ruff, M., Chambon, P., Gronemeyer, H., and Moras, D. (1995) *Nature* **375**, 377–382
11. Gampe, R. T., Jr., Montana, V. G., Lambert, M. H., Wisely, G. B., Milburn, M. V., and Xu, H. E. (2000) *Genes Dev.* **14**, 2229–2241
12. Egea, P. F., Mitschler, A., Rochel, N., Ruff, M., Chambon, P., and Moras, D. (2000) *EMBO J.* **19**, 2592–2601
13. Egea, P. F., Mitschler, A., and Moras, D. (2002) *Mol. Endocrinol.* **16**, 987–997
14. Nahoum, V., Pérez, E., Germain, P., Rodríguez-Barrios, F., Manzo, F., Kammerer, S., Lemaire, G., Hirsch, O., Royer, C. A., Gronemeyer, H., de Lera, A. R., and Bourguet, W. (2007) *Proc. Natl. Acad. Sci. U.S.A.* **104**, 17323–17328
15. Kersten, S., Pan, L., and Noy, N. (1995) *Biochemistry* **34**, 14263–14269
16. Altucci, L., Leibowitz, M. D., Ogilvie, K. M., de Lera, A. R., and Gronemeyer, H. (2007) *Nat. Rev. Drug Discov.* **6**, 793–810
17. Sakaki, J., Kishida, M., Konishi, K., Gunji, H., Toyao, A., Matsumoto, Y., Kanazawa, T., Uchiyama, H., Fukaya, H., Mitani, H., Arai, Y., and Kimura, M. (2007) *Bioorg. Med. Chem. Lett.* **17**, 4804–4807
18. Yotsumoto, T., Naitoh, T., Kanaki, T., and Tsuruzoe, N. (2005) *Metabolism* **54**, 573–578
19. Xu, H. E., Stanley, T. B., Montana, V. G., Lambert, M. H., Shearer, B. G., Cobb, J. E., McKee, D. D., Galardi, C. M., Plunket, K. D., Nolte, R. T., Parks, D. J., Moore, J. T., Kliewer, S. A., Willson, T. M., and Stimmel, J. B. (2002) *Nature* **415**, 813–817
20. Zhang, L., Liu, W., Hu, T., Du, L., Luo, C., Chen, K., Shen, X., and Jiang, H. (2008) *J. Biol. Chem.* **283**, 5370–5379
21. Otwinowski, Z., and Minor, W. (1997) *Methods Enzymol.* **276**, 307–326
22. Collaborative Computational Project Number 4 (1994) *Acta Crystallogr. D Biol. Crystallogr.* **50**, 760–763
23. Brünger, A. T., Adams, P. D., Clore, G. M., DeLano, W. L., Gros, P., Grosse-Kunstleve, R. W., Jiang, J. S., Kuszewski, J., Nilges, M., Pannu, N. S., Read, R. J., Rice, L. M., Simonson, T., and Warren, G. L. (1998) *Acta Crystallogr. D Biol. Crystallogr.* **54**, 905–921
24. Emsley, P., and Cowtan, K. (2004) *Acta Crystallogr. D Biol. Crystallogr.* **60**, 2126–2132
25. Laskowski, R. A., MacArthur, M. W., Moss, D. S., and Thornton, J. M. (1993) *J. Appl. Cryst.* **26**, 283–291
26. DeLano, W. L. (2002) *The PyMOL Molecular Graphics System*, DeLano Scientific LLC, San Carlos, CA
27. Brzozowski, A. M., Pike, A. C., Dauter, Z., Hubbard, R. E., Bonn, T., Engström, O., Ohman, L., Greene, G. L., Gustafsson, J. A., and Carlquist, M. (1997) *Nature* **389**, 753–758
28. Schoch, G. A., D'Arcy, B., Stihle, M., Burger, D., Bär, D., Benz, J., Thoma, R., and Ruf, A. (2010) *J. Mol. Biol.* **395**, 568–577
29. Bourguet, W., Vivat, V., Wurtz, J. M., Chambon, P., Gronemeyer, H., and Moras, D. (2000) *Mol. Cell* **5**, 289–298
30. Chen, J. D., and Evans, R. M. (1995) *Nature* **377**, 454–457
31. Jackson, T. A., Richer, J. K., Bain, D. L., Takimoto, G. S., Tung, L., and Horwitz, K. B. (1997) *Mol. Endocrinol.* **11**, 693–705
32. Kersten, S., Reczek, P. R., and Noy, N. (1997) *J. Biol. Chem.* **272**, 29759–29768
33. Huang, Q., Lu, G., Shen, H. M., Chung, M. C., and Ong, C. N. (2007) *Med. Res. Rev.* **27**, 609–630
34. Gao, Q., Qin, W. S., Jia, Z. H., Zheng, J. M., Zeng, C. H., Li, L. S., and Liu, Z. H. (2010) *Planta Med.* **76**, 27–33
35. Liu, Y., Jia, L., Liu, Z. C., Zhang, H., Zhang, P. J., Wan, Q., and Wang, R. (2009) *Exp. Mol. Med.* **41**, 648–655
36. Xue, J., Ding, W., and Liu, Y. (2010) *Fitoterapia* **81**, 173–177